

March 13, 2023
**Delone lattice studies in \mathbf{C}^3 , the space of three complex
 variables**

LAWRENCE C. ANDREWS^{a*} AND HERBERT J. BERNSTEIN^b

^a*Ronin Institute, 9515 NE 137th St, Kirkland, WA, 98034-1820 USA, and* ^b*Ronin
 Institute, c/o NSLS-II, Brookhaven National Laboratory, Upton, NY, 11973 USA.*

E-mail: lawrence.andrews@ronininstitute.org

lattice; reduction; Delone; Selling; \mathbf{C}^3

Abstract

The Delone (Selling) scalars, which are used in unit cell reduction and in lattice type determination, are studied in \mathbf{C}^3 , the space of three complex variables. The three complex coordinate planes are composed of the six Delone scalars. The transformations at boundaries of the Selling reduced orthant are described as matrices of operators. A graphical representation as the projections onto the three coordinates is described.

Note: In his later publications, Boris Delaunay used the Russian version of his surname, Delone.

1. Introduction

The scalars used by Delaunay (1932) in his formulation of Selling reduction (Selling, 1874) are (in the conventional order) $b \cdot c$, $a \cdot c$, $a \cdot b$, $a \cdot d$, $b \cdot d$, $c \cdot d$, where $d = -a - b - c$.

(As a mnemonic device, observe that the first three terms use α , β , and γ , in that order, and the following terms use a , b , c , in that order.)

Andrews et al. (2019b) chose to represent the Selling scalars in the space \mathbf{S}^6 , $\{s_1, s_2, s_3, s_4, s_5, s_6\}$ (defined in the order above), as a way to create a metric space for the measurement of the distance between lattices. They also considered the representation of this space as the space of three complex dimensions, \mathbf{C}^3 or $\{c_1, c_2, c_3\}$.

In \mathbf{C}^3 , in terms of the Selling scalars, a vector is defined as $\{(s_1, s_4), (s_2, s_5), (s_3, s_6)\}$, where the real and imaginary parts of each are the “opposite” scalars according to the definition of Delaunay (1932) (opposite in terms of the Bravais tetrahedron of scalars) (see Andrews et al. (2019a)). As a mnemonic device, note that the complex components involve (α, a) , (β, b) , and (γ, c) . Additionally, each complex term uses all four three-space vectors; for example, c_1 is $(b \cdot c, a \cdot d)$.

Andrews et al. (2019b) considered the matrix representations of the reflections in \mathbf{C}^3 (and in \mathbf{S}^6). This paper describes the boundary transformations at the edges of the fundamental unit of \mathbf{C}^3 and also a graphical presentation. In \mathbf{S}^6 , the fundamental unit is the all negative orthant, which contains only, and all of, the reduced cells. In \mathbf{S}^6 and \mathbf{C}^3 , the boundaries located where any \mathbf{S}^6 scalar (or correspondingly in \mathbf{C}^3 , a real or imaginary part) equals zero.

2. Notation

Complex numbers are represented in Cartesian format (x, y) , where x is the real part and y is the imaginary part.

We represent a vector in \mathbf{C}^3 by $\{(x_1, y_1), (x_2, y_2), (x_3, y_3)\}$ as an alternative to $\{(s_1, s_4), (s_2, s_5), (s_3, s_6)\}$.

Next we define the operators in \mathbf{C}^3 that will be used in the matrix descriptions of the transformations at the boundaries of the fundamental unit, see Table 1.

Table 1. *The Result column values give the products of each operator as applied to (x_j, y_j)*

Operator	Usage	Result	Name
\mathfrak{M}_r	$\mathfrak{M}_r(c_j)$	$(-x_j, -x_j + y_j)$	Minus real
\mathfrak{M}_i	$\mathfrak{M}_i(c_j)$	$(x_j - y_j, -y_j)$	Minus imag
\mathfrak{P}_r	$\mathfrak{P}_r(c_j)$	(x_j, x_j)	Plus real
\mathfrak{P}_i	$\mathfrak{P}_i(c_j)$	(y_j, y_j)	Plus imag
\mathfrak{R}	$\mathfrak{R}(c_j)$	x_j	Real
\mathfrak{I}	$\mathfrak{I}(c_j)$	y_j	Imaginary

3. Matrices of boundary transformations

For the boundary at s_1 : (the real component of c_1).

$$\begin{bmatrix} \mathfrak{M}_r & 0 & 0 \\ \mathfrak{P}_r & i\mathfrak{R} & \mathfrak{R} \\ \mathfrak{P}_r & i\mathfrak{I} & \mathfrak{I} \end{bmatrix} \begin{bmatrix} \mathfrak{M}_r & 0 & 0 \\ \mathfrak{P}_r & i\mathfrak{I} & \mathfrak{I} \\ \mathfrak{P}_r & i\mathfrak{R} & \mathfrak{R} \end{bmatrix} \begin{bmatrix} \mathfrak{M}_r & 0 & 0 \\ \mathfrak{P}_r & \mathfrak{R} & i\mathfrak{R} \\ \mathfrak{P}_r & \mathfrak{I} & i\mathfrak{I} \end{bmatrix} \begin{bmatrix} \mathfrak{M}_r & 0 & 0 \\ \mathfrak{P}_r & \mathfrak{I} & i\mathfrak{I} \\ \mathfrak{P}_r & \mathfrak{R} & i\mathfrak{R} \end{bmatrix}$$

For the boundary at s_4 : (the imaginary component of c_1).

$$\begin{bmatrix} \mathfrak{M}_i & 0 & 0 \\ \mathfrak{P}_i & i\mathfrak{R} & \mathfrak{R} \\ \mathfrak{P}_i & i\mathfrak{I} & \mathfrak{I} \end{bmatrix} \begin{bmatrix} \mathfrak{M}_i & 0 & 0 \\ \mathfrak{P}_i & i\mathfrak{I} & \mathfrak{I} \\ \mathfrak{P}_i & i\mathfrak{R} & \mathfrak{R} \end{bmatrix} \begin{bmatrix} \mathfrak{M}_i & 0 & 0 \\ \mathfrak{P}_i & \mathfrak{R} & i\mathfrak{R} \\ \mathfrak{P}_i & \mathfrak{I} & i\mathfrak{I} \end{bmatrix} \begin{bmatrix} \mathfrak{M}_i & 0 & 0 \\ \mathfrak{P}_i & \mathfrak{I} & i\mathfrak{I} \\ \mathfrak{P}_i & \mathfrak{R} & i\mathfrak{R} \end{bmatrix}$$

For the boundary at s_2 (the real component of c_2):

$$\begin{bmatrix} i\mathfrak{R} & \mathfrak{P}_r & \mathfrak{R} \\ 0 & \mathfrak{M}_r & 0 \\ i\mathfrak{I} & \mathfrak{P}_r & \mathfrak{I} \end{bmatrix} \begin{bmatrix} i\mathfrak{I} & \mathfrak{P}_r & \mathfrak{I} \\ 0 & \mathfrak{M}_r & 0 \\ i\mathfrak{R} & \mathfrak{P}_r & \mathfrak{R} \end{bmatrix} \begin{bmatrix} \mathfrak{R} & \mathfrak{P}_r & i\mathfrak{R} \\ 0 & \mathfrak{M}_r & 0 \\ \mathfrak{I} & \mathfrak{P}_r & i\mathfrak{I} \end{bmatrix} \begin{bmatrix} \mathfrak{I} & \mathfrak{P}_r & i\mathfrak{I} \\ 0 & \mathfrak{M}_r & 0 \\ \mathfrak{R} & \mathfrak{P}_r & i\mathfrak{R} \end{bmatrix}$$

For the boundary at s_5 : (the imaginary component of c_2).

$$\begin{bmatrix} i\mathfrak{R} & \mathfrak{P}_i & \mathfrak{R} \\ 0 & \mathfrak{M}_i & 0 \\ i\mathfrak{I} & \mathfrak{P}_i & \mathfrak{I} \end{bmatrix} \begin{bmatrix} i\mathfrak{I} & \mathfrak{P}_i & \mathfrak{I} \\ 0 & \mathfrak{M}_i & 0 \\ i\mathfrak{R} & \mathfrak{P}_i & \mathfrak{R} \end{bmatrix} \begin{bmatrix} \mathfrak{R} & \mathfrak{P}_i & i\mathfrak{R} \\ 0 & \mathfrak{M}_i & 0 \\ \mathfrak{I} & \mathfrak{P}_i & i\mathfrak{I} \end{bmatrix} \begin{bmatrix} \mathfrak{I} & \mathfrak{P}_i & i\mathfrak{I} \\ 0 & \mathfrak{M}_i & 0 \\ \mathfrak{R} & \mathfrak{P}_i & i\mathfrak{R} \end{bmatrix}$$

For the boundary at s_3 (the real component of c_3):

$$\begin{bmatrix} i\mathfrak{R} & \mathfrak{R} & \mathfrak{P}_r \\ i\mathfrak{I} & \mathfrak{I} & \mathfrak{P}_r \\ 0 & 0 & \mathfrak{M}_r \end{bmatrix} \begin{bmatrix} i\mathfrak{I} & \mathfrak{I} & \mathfrak{P}_r \\ i\mathfrak{R} & \mathfrak{R} & \mathfrak{P}_r \\ 0 & 0 & \mathfrak{M}_r \end{bmatrix} \begin{bmatrix} \mathfrak{R} & i\mathfrak{R} & \mathfrak{P}_r \\ \mathfrak{I} & i\mathfrak{I} & \mathfrak{P}_r \\ 0 & 0 & \mathfrak{M}_r \end{bmatrix} \begin{bmatrix} \mathfrak{I} & i\mathfrak{I} & \mathfrak{P}_r \\ \mathfrak{R} & i\mathfrak{R} & \mathfrak{P}_r \\ 0 & 0 & \mathfrak{M}_r \end{bmatrix}$$

For the boundary at s_6 (the imaginary component of c_3):

$$\begin{bmatrix} i\Re & \Re & \Im_i \\ i\Im & \Im & \Re_i \\ 0 & 0 & \Re_i \end{bmatrix} \begin{bmatrix} i\Im & \Im & \Re_i \\ i\Re & \Re & \Im_i \\ 0 & 0 & \Re_i \end{bmatrix} \begin{bmatrix} \Re & i\Re & \Re_i \\ \Im & i\Im & \Re_i \\ 0 & 0 & \Re_i \end{bmatrix} \begin{bmatrix} \Im & i\Im & \Re_i \\ \Re & i\Re & \Re_i \\ 0 & 0 & \Re_i \end{bmatrix}$$

4. Basics

The standard representation of the identity operation is

$$\mathbf{c}' = \begin{bmatrix} 1 & 0 & 0 \\ 0 & 1 & 0 \\ 0 & 0 & 1 \end{bmatrix} \mathbf{c}.$$

The identity in \mathbf{C}^3 can also be written:

$$\mathbf{c}' = \begin{bmatrix} 1 & 0 & 0 \\ 0 & \Re + i\Im & 0 \\ 0 & 0 & \Re + i\Im \end{bmatrix} \mathbf{c}.$$

Delaunay (1932) does not consider the boundary transformations in detail. However, he uses them to define the process of Selling reduction. For example in \mathbf{S}^6 , he lists the following as one of the possible results for a transformation on s_1 , translated to \mathbf{S}^6 : $\{-s_1, -s_1+s_2, s_1+s_3, s_1+s_5, s_1+s_4, s_1+s_6\}$. The third boundary transform for s_1 above implements this operation and interchanges the real part of c_3 and the imaginary part of c_2 :

$$\begin{bmatrix} \Re_r & 0 & 0 \\ \Im_r & \Re & i\Re \\ \Re_r & \Im & i\Im \end{bmatrix}$$

Considered in \mathbf{C}^3 , Delone's alternate transformation for the s_1 boundary would exchange the real of c_2 with the imaginary part of c_3 . That is the fourth matrix above in the list for s_1 . The other two transformations for s_1 can be generated from the two we have just mentioned by the “exchange operation” (Andrews et al., 2019b) applied to the second and third \mathbf{C}^3 coordinates. Delone did not describe the latter

two transformations, perhaps because even a single transformation was adequate to implement reduction. He had already listed two.

5. Graphical display of projections

The two-dimensional nature of the three coordinates of \mathbf{C}^3 suggests their use for graphical display.

As an example, we use Phospholipase A2 (**PLA2**) (retrieved from the Protein Data Bank (Bernstein et al., 1977)), which has had several similar or identical structures determined (Le Trong & Stenkamp, 2007). Andrews et al. (2019b) found additional cases (see Table 2)

PDB id	Centering	a	b	c	α	β	γ
1DPY	R	57.98	57.98	57.98	92.02	92.02	92.02
1FE5	R	57.98	57.98	57.98	92.02	92.02	92.02
1G0Z	H	80.36	80.36	99.44	90	90	120
1G2X	C	80.95	80.57	57.1	90	90.35	90
1U4J	H	80.36	80.36	99.44	90	90	120
2OSN	R	57.10	57.10	57.10	89.75	89.75	89.75

Table 2. *Phospholipase A2 unit cells*

Below, Figure 1 shows the unit cells as reported (the centering of lattices has not been removed). The following figures (Figures 2 to 5) show various transformations and embellishments of the reported cells.

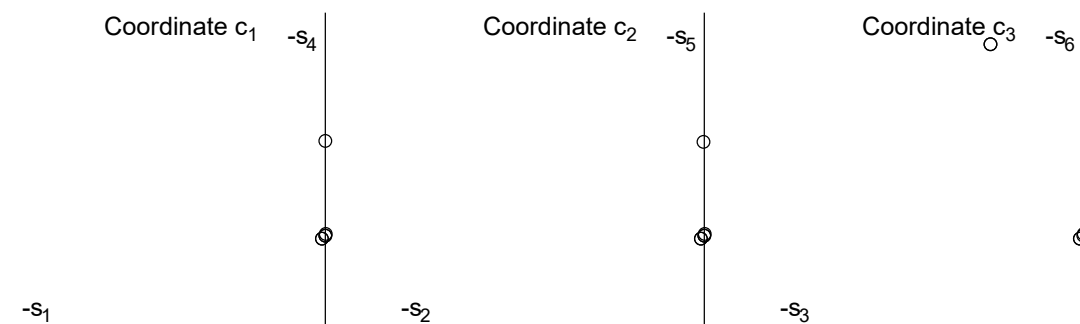


Fig. 1. Phospholipase A2 unit cells as reported.

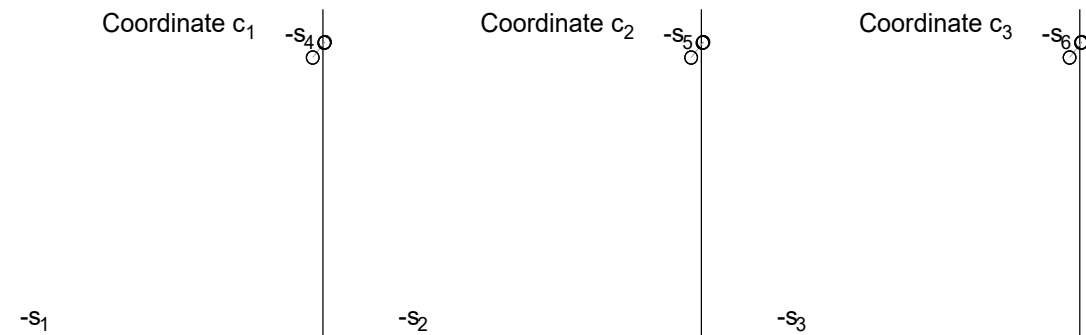


Fig. 2. The PLA2 unit cells Niggli-reduced. The similarity of the 3 projections is indicative of the exact or nearly exact rhombohedral symmetry.

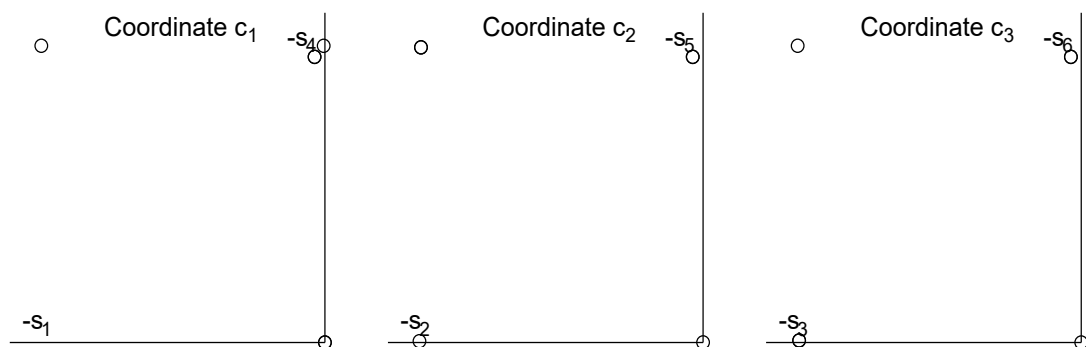


Fig. 3. The PLA2 unit cells Delone-reduced.

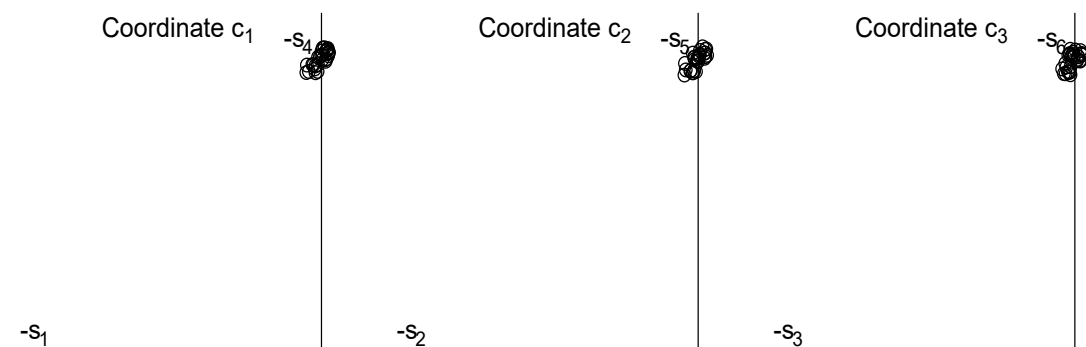


Fig. 4. The PLA2 unit cells, Niggli-reduced, and five copies were perturbed 2% orthogonally to \mathbf{S}^6 vector.

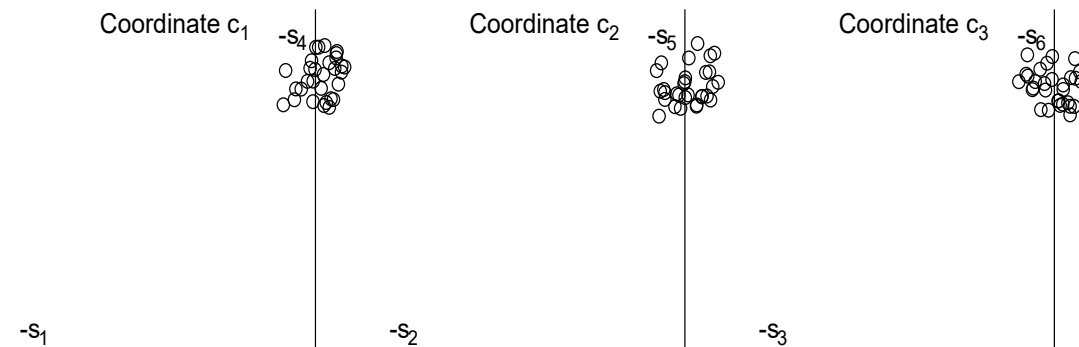


Fig. 5. The PLA2 unit cells, Niggli-reduced, and five copies were perturbed 10% orthogonally to \mathbf{S}^6 vector.

6. Summary

The transformation matrices shown above demonstrate the considerable regularity of Selling reduction, as used by Delaunay (1932). The reduction operations of Niggli reduction (Niggli, 1928) are more complex. While all the boundaries of the non-positive orthant of \mathbf{S}^6 are essentially the same (and related by reflections), the boundaries formed in Niggli reduction are of multiple types, and the fundamental unit of the space representing Niggli-reduced cells (\mathbf{G}^6 , see Andrews & Bernstein (2014)) is non-convex.

Several aspects of \mathbf{C}^3 are evident from inspecting the matrices. First, each boundary has four possible transformations that can be applied. Since each of the transformations at boundaries are self-inverse, they are the same transformations that would be used in the process of cell (lattice) reduction. Delaunay (1932) and Delone *et al.* (1975) give only two choices, presumably for simplicity, omitting transformations that use the “exchange” operator (see Andrews *et al.* (2019b)).

7. Availability of code

The C^{++} code for \mathbf{C}^3 and related software tools is available in github.com, in <https://github.com/duck10/LatticeRepLib.git>.

Acknowledgements

Careful copy-editing and corrections by Frances C. Bernstein are gratefully acknowledged. Our thanks to Jean Jakoncic and Alexei Soares for helpful conversations and access to data and facilities at Brookhaven National Laboratory.

Funding information

Funding for this research was provided in part by: US Department of Energy Offices of Biological and Environmental Research and of Basic Energy Sciences (grant No. DE-AC02-98CH10886; grant No. E-SC0012704); U.S. National Institutes of Health (grant No. P41RR012408; grant No. P41GM103473; grant No. P41GM111244; grant No. R01GM117126, grant No. 1R21GM129570); Dectris, Ltd.

References

- Andrews, L. C. & Bernstein, H. J. (2014). The geometry of niggli reduction: Bgaol-embedding niggli reduction and analysis of boundaries. *J. Appl. Cryst.* **47**(1), 346 – 359.
- Andrews, L. C., Bernstein, H. J. & Sauter, N. K. (2019a). Selling reduction versus Niggli reduction for crystallographic lattices. *Acta Cryst.* **A75**(1), 115 – 120.
- Andrews, L. C., Bernstein, H. J. & Sauter, N. K. (2019b). A space for lattice representation and clustering. *Acta Cryst.* **A75**(3), 593–599.
- Bernstein, F. C., Koetzle, T. F., Williams, G. J. B., Meyer, Jr., E. F., Brice, M. D., Rodgers, J. R., Kennard, O., Shimanouchi, T. & Tasumi, M. (1977). The Protein Data Bank: a computer-based archival file for macromolecular structures. *J. Mol. Biol.* **112**, 535 – 542.
- Delaunay, B. N. (1932). Neue Darstellung der geometrischen Kristallographie. *Z. Krist.* **84**, 109 – 149.
- Delone, B. N., Galiulin, R. V. & Shtogrin, M. I. (1975). On the Bravais types of lattices. *J. Sov. Math.* **4**(1), 79 – 156.
- Le Trong, I. & Stenkamp, R. E. (2007). An alternate description of two crystal structures of phospholipase a2 from *bungarus caeruleus*. *Acta Cryst.* **D63**(4), 548 – 549.
- Niggli, P., (1928). Krystallographische und Strukturtheoretische Grundbegriffe, Handbuch der Experimentalphysik, Vol. 7, part 1. Akademische Verlagsgesellschaft, Leipzig.
- Selling, E. (1874). Über die binären und ternären quadratischen formen. *Journal für die reine und angewandte Mathematik (Crelle's Journal)*, **1874**(77), 143 – 229.

Synopsis

The space \mathbf{C}^3 is explained in more detail than in the original description. Boundary transformations of the fundamental unit are described in detail. A graphical presentation of the basic coordinates is described and illustrated.
